

Northumbria Research Link

Citation: Buri, Pascal and Pellicciotti, Francesca (2018) Aspect controls the survival of ice cliffs on debris-covered glaciers. Proceedings of the National Academy of Sciences of the United States of America, 115 (17). pp. 4369-4374. ISSN 0027-8424

Published by: National Academy of Sciences

URL: <http://dx.doi.org/10.1073/pnas.1713892115>
<<http://dx.doi.org/10.1073/pnas.1713892115>>

This version was downloaded from Northumbria Research Link:
<http://nrl.northumbria.ac.uk/id/eprint/34249/>

Northumbria University has developed Northumbria Research Link (NRL) to enable users to access the University's research output. Copyright © and moral rights for items on NRL are retained by the individual author(s) and/or other copyright owners. Single copies of full items can be reproduced, displayed or performed, and given to third parties in any format or medium for personal research or study, educational, or not-for-profit purposes without prior permission or charge, provided the authors, title and full bibliographic details are given, as well as a hyperlink and/or URL to the original metadata page. The content must not be changed in any way. Full items must not be sold commercially in any format or medium without formal permission of the copyright holder. The full policy is available online: <http://nrl.northumbria.ac.uk/policies.html>

This document may differ from the final, published version of the research and has been made available online in accordance with publisher policies. To read and/or cite from the published version of the research, please visit the publisher's website (a subscription may be required.)



**Northumbria
University**
NEWCASTLE



UniversityLibrary

Aspect controls the survival of ice cliffs on debris-covered glaciers

Pascal Buri^{a,1} and Francesca Pellicciotti^b

^aInstitute of Environmental Engineering, Hydrology and Water Resources Management Group, ETH Zürich, Stefano-Franscini-Platz 3, 8093 Zürich, Switzerland; ^bFaculty of Engineering and Environment, Department of Geography, Northumbria University, Ellison Building, Newcastle upon Tyne, NE18ST, UK

This manuscript was compiled on March 7, 2018

Supraglacial ice cliffs exist on debris-covered glaciers worldwide, but despite their importance as melt hot spots their life cycle is little understood. Early field observations had advanced a hypothesis of survival of north-facing and disappearance of south-facing cliffs which is central for predicting the contribution of cliffs to total glacier mass losses. Their role as windows of energy transfer suggests they may explain the anomalously high mass losses of debris-covered glaciers in High Mountain Asia (HMA) despite the insulating debris, currently at the centre of a debated controversy. We use a 3D model of cliff evolution coupled to very high resolution topographic data to demonstrate that ice cliffs facing south (in the Northern Hemisphere) disappear within few months due to enhanced solar radiation receipts, and that aspect is the key control on cliffs evolution. We reproduce continuous flattening of south-facing cliffs, a result of their vertical gradient of incoming solar radiation and sky view factor. Our results establish that only north-facing cliffs are recurrent features and thus stable contributors to the melting of debris-covered glaciers. Satellite observations and mass balance modelling confirms that few south-facing cliffs of small size exist on the glaciers of Langtang, and their contribution to the glacier volume losses is very small (~1%). This has major implications for the mass balance of HMA debris-covered glaciers as it provides the basis for new parameterisations of cliff evolution and distribution to constrain volume losses in a region where glaciers are highly relevant as water sources for millions of people.

debris-covered glaciers | supraglacial ice cliffs | energy-balance modelling | cliff evolution | High Mountain Asia

Many glacier tongues in High Mountain Asia are heavily debris-covered (1, 2). Despite the insulating effect of a mantle composed by rock debris on the underlying ice (3, 4), large-scale, satellite-based studies have suggested that thinning rates of debris-covered glaciers are comparable to those of clean ice glaciers (5, 6). Although recent studies at the catchment and glacier scale do not support analogous thinning (7, 8), it has by now been established that strong local increases in glacier ablation are associated with supraglacial ponds and cliffs (9–12). Cliffs forming on the surface of debris-covered glaciers contribute to the glacier mass balance through enhanced melt rates, but also affect glacier dynamics, and knowledge about their life cycle and distribution is important to predict future evolution of debris-covered glaciers (13). The understanding of processes acting at the scale of single cliffs has been dramatically improved recently through modelling approaches that have simulated energy fluxes and melt (11, 14) and estimated volume losses (15) of single cliffs. The rate at which cliffs can affect glacier mass balance and dynamics depends on their distribution and persistence in time, but how cliffs form, evolve and decline is not yet understood, precluding a holistic understanding of their role on longer

term mass balance patterns beyond the few observations over a melt season. A hypothesis of persisting north-facing and disappearing south-facing cliffs has been first proposed more than one decade ago (16) based on observations and conceptual assumptions on the importance of solar radiation on ice cliff melt (17, 18). The hypothesis seems to be supported by inventories of cliff distribution from satellite observations of single or selected glaciers in the Khumbu region (Nepalese Himalaya) (12, 19). Conceptual intuition, supported by sparse observational evidence, has postulated that cliff faces oriented to the south are reburied rapidly and do not persist over debris-covered glaciers, independently of glacier flow direction. No study, however, has been able so far to explain the absence of south-facing cliffs on debris-covered glaciers.

Backwasting of south-facing cliffs

Here, we simulate the evolution of south-facing ice cliffs to understand the effect of enhanced solar radiation compared to observed north-facing cliffs. Our aim is to establish whether south-facing supraglacial cliffs persist beyond the length of a melt season, as observed northerly-facing cliffs do, or if they disappear more rapidly, and to identify the causes for their behaviour. To test this, we run a 3D numerical model of cliff backwasting that was able to reproduce the evolution of north-facing cliffs (14). We force the model with hourly meteorological data from an on-glacier automatic weather station (AWS) (20) and initialise it with a digital elevation

Significance Statement

Glaciers in High Mountain Asia (HMA) are *important* water sources for millions of people downstream. Ice cliffs on debris-covered glaciers act as hot spots for melt and *may explain anomalously high* glacier mass losses in HMA, but their temporal evolution remains unknown, hindering sound parameterisations of these features in glacier models. We simulate the evolution of cliff systems with different aspects, *show that south-facing* ice cliffs disappear within a few weeks *in the Northern Hemisphere* and for the first time explain the processes driving this. *Cliffs that persist melt ten times faster than the surrounding glacier surfaces. These findings provide a new basis for understanding the surface evolution of debris-covered glaciers with implications for their dynamics, mass balance and hydrology.*

F.P. and P.B. designed research. P.B. performed simulations. P.B. and F.P. analyzed data and wrote the paper.

The authors declare no conflict of interest.

¹To whom correspondence should be addressed. E-mail: buri@ifu.baug.ethz.ch

model (DEM) (21) of sub-metre resolution over the debris-covered Lirung Glacier (Nepalese Himalaya, Fig. 1a).

Initial conditions for our simulations were created by rotating north-facing ice cliff topographies as observed on Lirung Glacier (Fig. 1b) towards south, including the surrounding glacier surface and ponds (Fig. 1c). Hence, the artificially derived south-facing cliffs were embedded into a realistic cliff-glacier topography and therefore directly comparable to the north-facing cliffs in terms of size, shape and surrounding topography. We applied a dynamic, physically-based backwasting model (14) on the two rotated cliffs over one ablation season (May to October 2013). Cliff melt is derived from distributed surface energy balance calculations and shapes the cliff surface by bi-weekly geometry updates. Melt at water-contact zones is enhanced to account for thermo-erosion by adjacent supraglacial ponds (10, 11). Depending on the slope and the amount of debris cells seen at the cliff margins, the cliffs can expand or shrink (because of reburial by debris).

We simulate continuous shrinkage of the south-facing cliffs, resulting in a significant reduction in extent after just a few weeks already (Fig. 2a). This is a striking difference compared to the evolution of the original north-facing cliffs (observed in the field and confirmed by our simulations (14)), shown in the background of Fig. 2a, which backwaste maintaining a self-similar geometry that allows the cliffs to persist until the end of the ablation season. The reason for the rapid shrinking of the south-facing cliffs is the progressive flattening of their surface (Fig. 2b), which allows reburial by debris. The complete reburial of the debris-free cliff areas occur after less than three (Cliff 1) to five months (Cliff 2, Tab. S2). Even when the cliff is not entirely reburied, large sections of its surface disappear, reducing consistently the area available for melt (Fig. 3c). In contrast, the north-facing cliffs show stable profiles backwasting with a constant slope (Cliff 2) or only minimal regrading (Cliff 1, Fig. 2b).

Radiative forcing at the cliff surface

To understand what controls the simulated cliffs' evolution, we rotated cliffs 1 and 2 together with their surrounding topography by increments of 45° from north into eight additional directions and modelled the seasonal surface energy balances. We then calculated diurnal cycles of the spatially-averaged energy fluxes for the rotated cliff surfaces (Fig. 3a-b and Supplementary information, Fig. S4 and S5) and spatial totals of energy fluxes and melt energy (Fig. 4, S6 and S7).

The longwave radiation component, comprised of radiation emitted by the debris surfaces around the cliff and of the longwave radiation emitted by the atmosphere, shows no aspect-related differences in amount and timing (Fig. S4e-f and S7a-b). This is not surprising as these fluxes depend on the surface (debris) and air (atmosphere) temperatures, which have no obvious dependence on aspect, and on the local topographical horizons (which are approximately constant for all directions). In contrast, a very high aspect-dependence is evident for the simulated shortwave radiation and its direct component in particular (Fig. 3a,c, 4a,c). Differences between directions are evident in both the timing and total amount of solar energy received. East-facing cliffs receive direct solar radiation earliest in the day, followed by south- and west-oriented slopes (Fig. 3a and 4a). The lowest amounts are received by cliffs with aspects in the range north to south-

west (Fig. 3a,c). East- and southeast-facing cliffs receive the highest direct solar radiation (up to 67% more than the original cliff and exceeding by 3.6 times the energy input at the northwest-facing cliff (Tab. S1)), followed by south-facing ones. These cliffs do not survive the duration of the ablation season, but disappear or undergo a substantial loss in area (Fig. 3c, Tab. S2). The apparently anomalous behaviour of south- and southwest-facing cliffs, which receive as little radiation as those with a prevalent northerly aspect, is likely due to the presence of cloud cover in the afternoon. During the ablation season, which coincides with the monsoon in this region, in the afternoon, when the south-facing cliffs are theoretically exposed to high solar radiation receipts, thick clouds and rain prevail with regularity and prevent high solar radiation incomes in the Langtang Valley (22, 23). This decreases the solar radiation receipt of southwesterly aspects considerably (18) and therefore dampens the all-year average of incoming shortwave energy (Fig. 3). The daily cycle and spatial patterns of melt energy closely reflect those of the solar radiation inputs, with the highest amount of melt energy for east- and southeast-facing cliffs (Fig. 3b and 4b). As a result of the energy forcing, cliffs with aspect in the range east to southwest do not survive, while cliffs facing northeast to west do (Fig. 3c, Tab. S2).

Spatial variability in solar radiation and melt energy is high over a single cliff (coefficients of variation for direct shortwave radiation up to 238% at the west-oriented surface of Cliff 2, Tab. S3). Solar radiation is highest at the top of the cliff, and this effect is stronger at noon because of the high sun angle (Fig. 4a). The top sections of the cliffs receive also the highest amount of atmospheric longwave radiation (Fig. S7b), thus amplifying the solar radiation control. This cannot be counterbalanced by the longwave flux emitted by the debris surface surrounding the slopes, which is highest at the cliffs margins (Fig. S7a). Total melt energy results from the interactions of these spatially variable fluxes and their temporal variability: it is highest at the top of the cliff (Fig. 4b) for most aspects, and decreases towards the cliffs bottom. This energy gradient is small (with minimum differences between the energy at the top and bottom of the cliff) for cliffs with northwest and western aspects (Fig. 4d, Tab. S3). These are those that survive (Fig. 3c) because a rather uniform distribution of solar radiation and melt energy allows their backwasting and maintenance of a constant steep slope, rather than downwasting and reburial by debris. The flux of energy emitted by the surrounding debris and received by the cliff margins is not high enough to counterbalance the atmospheric fluxes of shortwave and longwave radiation at south-oriented cliffs. High receipts of solar radiation at the top of these cliffs cause a progressive flattening. The cliff flattening, controlled by the sky view factor and hence the amount of sky that the cliff sections are exposed to, is thus strongly aspect-dependent. Longitudinal profiles of progressively higher solar radiation amounts from base to top will have a much stronger vertical gradient for those aspects that receive much higher solar radiation in the morning hours (northeast to southeast). The upper part of Cliff 2 shows a 20–30% higher sky view factor compared to the base zone (Fig. S8c). The reduction in sky-openness towards the cliff bottom is the combined result of the topography in front of the cliff face and the steep slopes at the cliff bottom. The combination of a very high shortwave

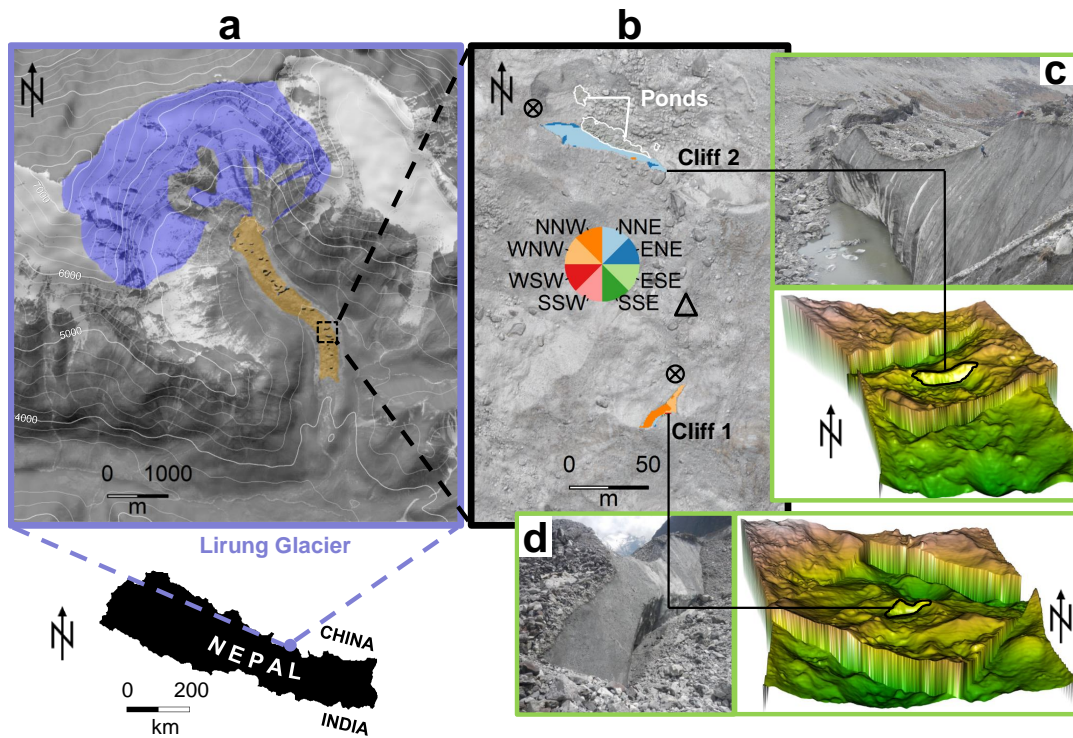


Fig. 1. Observed cliffs on Lirung Glacier, Langtang Valley, Nepalese Himalaya. (a) Lirung Glacier with debris covered tongue (orange) and accumulation area (violet). (b) Lirung Glacier surface around cliffs 1 and 2 (marked by colours indicating their aspect, and observed aspect of the cliff faces). Encircled crosses denote position where terrestrial images (c and d) were taken, triangle shows the location of the Automatic Weather Station (AWS). (c) Cliff 2 photographed from the location indicated in (b) (top) in May 2013, and rotated cliff system shown as 3D-elevation model (bottom). (d) Cliff 1 (left) as observed in a photo (taken from the location shown in (b) in May 2013, and rotated cliff system shown as 3D-elevation model (right). Background images: Orthoimage ALOS December 2010 and ASTER GDEM2 hillshade (a); Orthoimage UAV May 2013 and UAV DEM May 2013 hillshade (b); Picture E. Miles May 2013 and partly rotated UAV DEM May 2013 (c and d).

radiation income together with a decreasing sky view factor towards the cliff base cause the cliffs with southerly to easterly aspect to flatten progressively over time, as the upper section recedes at much higher rates than the lower parts, until they reach a slope that can be reburied by debris.

Discussion

Our model results show that south-facing supraglacial ice cliffs progressively shrink and disappear within a few weeks. We thus provide the first explanation for previous observations and conceptual suggestions that (in the Northern Hemisphere) cliffs with a southern aspect are not part of the cliff population on glacier surfaces, as they do not persist on time scales relevant for glacier mass balance considerations. This narrows the knowledge gap concerning distribution and evolution of cliffs as the population of cliff systems can be reduced to northerly to westerly-facing ones. We can explain this distribution with the enhanced solar radiation received by the cliffs with southern aspects. Southeast- and northwest-oriented cliffs are likely the extremes of cliff life expectancy, as exposure to solar radiation and shadowing, respectively, are highest for these aspects.

We have also further established that ice cliffs are melt hot spots that efficiently convey large amount of atmospheric energy into the glacier ice. The daily melt rates of the two ice cliffs vary between 4.6 (for northwest orientation) and 6.3cm (for east- and south-eastern orientations, Tab. S1) and exceed the observed daily sub-debris melt of 0.5cm on Lirung Glacier

(21) for the same period by about ten times. However, starting from very high melt rates for all cliff orientations (and for the predominantly north- and predominantly south-facing cliffs, their behaviour diverges significantly over the course of the melt season: on southerly facing cliffs the spatial distribution of the energy fluxes lead to the progressive flattening and disappearance of the cliffs (Fig. 2), while on northerly-facing cliffs the distinct interaction of cliff topography and energy distribution maintains self-consistent, persistent cliffs.

We are able to reproduce the flattening of southerly-facing cliffs induced by much higher direct solar radiation, compared to northerly-oriented cliffs, and the increase of the shortwave radiation-relevant sky view factor from cliff base to crest. The increasing debris view factor towards the cliff base (along a vertical gradient) and boundary zones (along a horizontal gradient from the cliff centre, Fig. S8d) results in a higher longwave radiation receipt from the surrounding debris at these cliff zones. This, however, is not able to counterbalance the extremely high solar radiation receipt of southerly aspects (as it is the case for cliff slopes facing north (11, 14, 20). Importantly, we have shown that the effect of adjacent ponds (which act on cliffs through enhanced melt through therm-erosion at the low-lying cliff-pond contact zone) is not sufficient to maintain southerly-facing cliffs steep and thus allow their persistence (Fig. 2b), as they are able to do for northerly-oriented cliffs (14). We show that there is a range of cliff aspects that determine their disappearance as a result of energy flux interaction and a range of aspects within which

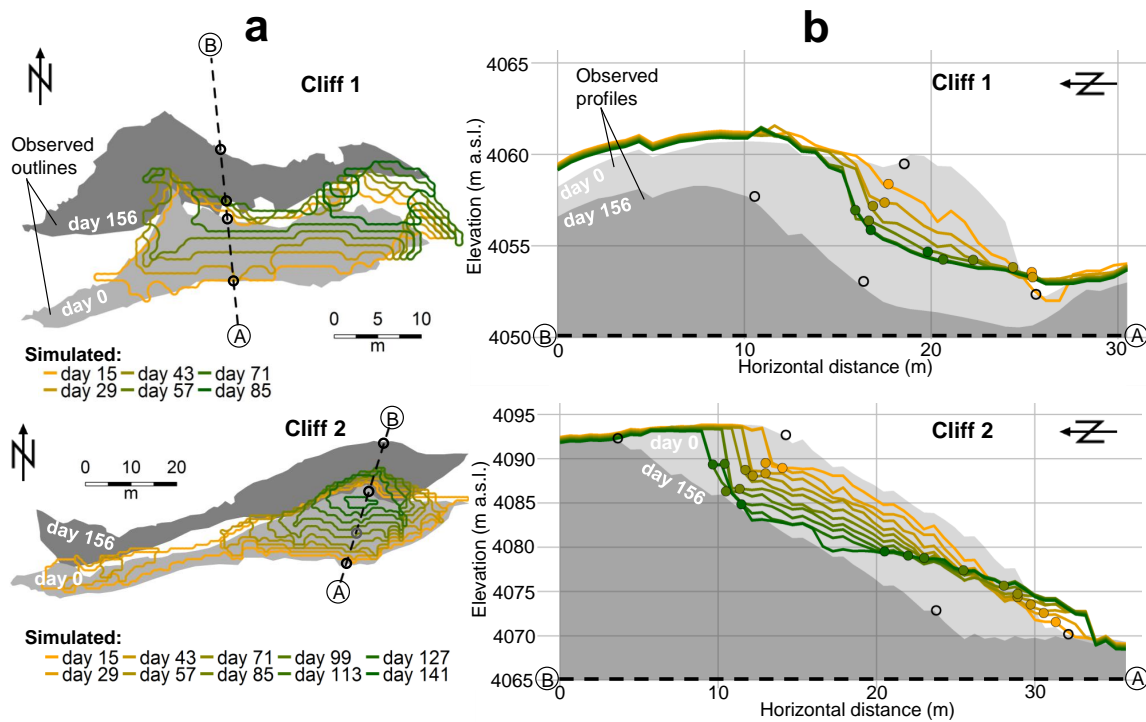


Fig. 2. Simulated outlines and elevation profiles of south-facing cliffs. (a) Cliffs 1 (top) and 2 (bottom) outlines simulated by the model with bi-weekly geometry updates (yellow to green lines). For comparison, also the observed shapes of north-facing cliffs are shown (light and dark grey polygons), rotated towards south for consistency. (The model was able to simulate the evolution of the original north-facing cliffs (14)). Dashed line indicates profile, thick circles the debris-ice transitions. (b) Elevation profiles of rotated cliffs 1 (top) and 2 (bottom) as simulated with bi-weekly geometry updates (yellow to green lines). Profiles of observed north-facing cliffs are also shown (light and dark grey areas), rotated towards south for consistency. Circles indicate debris-ice transitions of modelled (yellow to green) and observed (thick black) cliff profiles. The last of the coloured lines (darkest green) indicates the last cliff profile before the cliffs disappear. None of the two cliffs survives for the duration of the ablation season, disappearing after day 85 (Cliff 1) and day 141 (Cliff 2). Days are counted from the start of the simulations, on 19 May 2013.

cliffs over monsoon-dominated central Himalayan glaciers will survive over the melting season: aspects from northeast to west are associated with cliff persistence, and those from east to southwest with progressive flattening and disappearance (Fig. 3c).

To test our results, we manually mapped all cliffs and ponds from UAV images in May 2014 as well as from a terrestrial photogrammetry survey carried out in October 2014 on Lirung Glacier (15). Since the UAV-surveys cover only a portion of the glacier, we used a SPOT6-orthoimage from April 2014 (very close to the UAV survey of May 2014) for both Lirung Glacier and Langtang Glacier, the largest glacier in the valley (SI Fig. S10 and Methods). For Langtang Glacier, we additionally use UAV-imagery from May 2014 and October 2015 to map cliffs and lakes at very high resolution. There are no southerly-facing cliffs on Lirung Glacier in the portion covered by the UAV-survey in either May or October. There are a total of four *south-facing* cliffs on the entire Lirung Glacier in April 2014 (from the SPOT6-image), three on Langtang Glacier on the portion covered by the UAV in May 2014 and nine in total over the entire glacier in April 2014 (SI Figs. S12 and S14, and SI Tab. S6). All South-facing cliffs are very small, covering 0.01% of Lirung entire glacier in April 2014, 2.93% of the portion of Langtang covered by the UAV in May 2014 and 0.07% of the entire Langtang Glacier in April 2014. While cliffs cover a total of 1.29 % of the debris-covered area, only 5.14% of this total cliff area is made of southerly-facing cliffs (Tab. S6), with two orders of magnitude difference in

the extension of southerly-facing cliffs compared to the entire population (Tab. S6).

We also run the cliff model on all the cliffs on the two glaciers (Methods and Supplementary Information, SI, Section 5) to estimate their total contribution to the mass losses of the two glaciers for the period between May and October 2014. Cliffs are major contributors to total glacier mass losses (with contributions of 36.43 and 19.84% for Lirung and Langtang Glacier, respectively, relative to the debris-covered glacier area; Tab. S6). Southerly-facing cliffs, however, contribute only to a very small percentage of these mass losses (1.2% on Langtang Glacier and 0% on Lirung Glacier as all southerly-oriented cliffs disappear with the first geometry update; Tab. S6).

The glacier scale observational evidence and large-scale modelling confirm the main findings of our modelling experiment. Southerly-facing cliffs are very few on two of the main glaciers of Langtang Valley, both at the beginning and at the end of the ablation season (Figs. S11 and S12), suggesting that indeed southerly-facing cliffs do not form part of the population of stable cliffs on the glaciers of the Langtang catchment. The two glaciers differ in area, dynamics and elevation ranges, and while Lirung has a quasi-stagnant tongue, Langtang Glacier is much larger (40.2km²) and more active (7), suggesting that our results are largely independent of flow dynamics, at least within the range of velocities of the Langtang Valley glaciers (7, 24). It is not clear however how the south-facing cliffs form, for lack of a general understanding on the formation of cliffs in general. Our work has established how cliffs evolve and

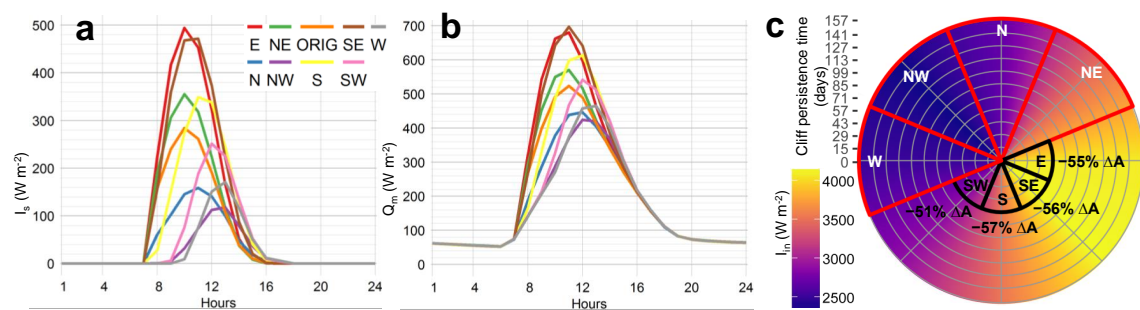


Fig. 3. Modelled surface energy fluxes for Cliff 2 rotated to various aspects. (a) Diurnal cycle (May–October 2013) of direct shortwave radiation receipt averaged in space over Cliff 2 rotated to eight different aspects by increments of 45° . (b) Diurnal cycle (May–October 2013) of melt energy averaged for Cliff 2 rotated to eight different aspects by increments of 45° . (c) Cliff persistence per aspect (angular scale in days, counted from the start of the simulations, on 19 May 2013); black lines indicate the time when more than 50% of the initially inclined area has disappeared (with ΔA indicated, providing the percentage of area that has disappeared at that time); red lines indicate the range of directions for which cliffs never reach that threshold (i.e. never loose more than 50% of their inclined area). Cliffs with aspects indicated in white (W, NW, N, NE) persisted for the entire season. In the background, the average daily sum of simulated incoming solar radiation per aspect is shown (blue to yellow).

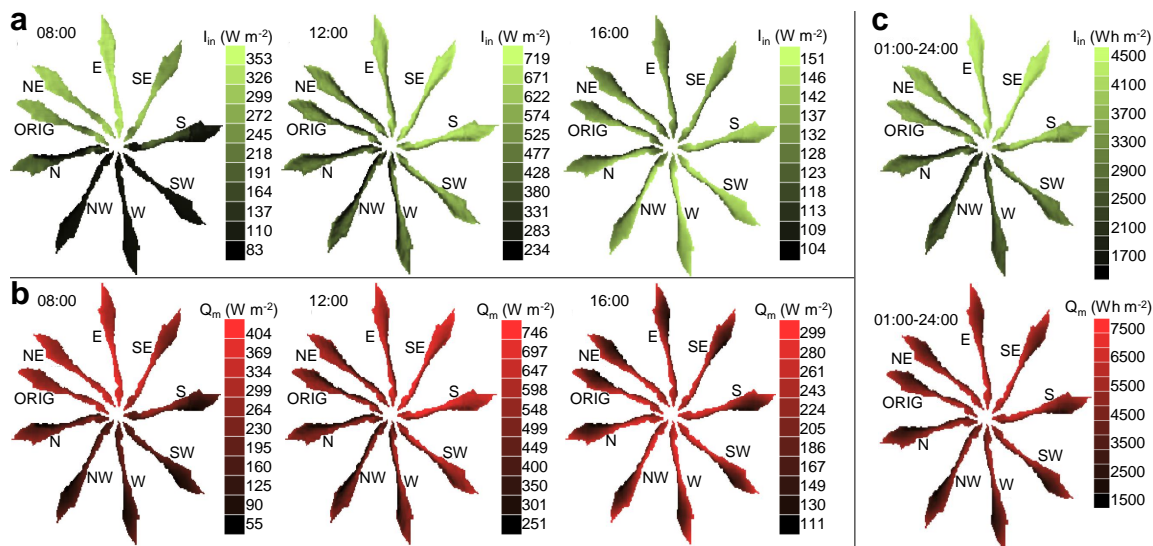


Fig. 4. Distributed energy fluxes modelled over Cliff 2 rotated to various aspects. (a) Distributed incoming shortwave radiation averaged over melt season (May–October 2013) rotated to eight different aspects by increments of 45° (indicated by label at crest of each cliff), shown for hours 8 (left), 12 (middle) and 16 (right) of the day, respectively. (b) Map of melt energy per pixel averaged over the melt season (May–October 2013) calculated over Cliff 2 rotated to eight different aspects by increments of 45° , shown for hours 8 (left), 12 (middle) and 16 (right) of the day, respectively. (c) Distributed daily sum (averaged May–October 2013) of incoming shortwave radiation. (d) Map of daily sums (averaged May–October 2013) of melt energy.

decay, and that the solar radiation received by a cliff and the shadowing of steep cliff surfaces is the first-order control of cliff melt, evolution and distribution. However, while radiation seems to ultimately control the evolution and disappearance of supraglacial ice cliffs, their appearance and the mechanisms controlling their formation are still largely unknown. Different hypotheses have been advanced, from subsurface developments such as collapsing of empty melt water channels close to the surface to surface changes induced by glacier dynamics or sub-debris melt (16, 25, 26), but none has been *demonstrated conclusively*. The picture is complicated by the fact that little is known on the distribution and characteristics of debris cover worldwide, and in HMA in particular. Initial observational and satellite evidence suggests that debris characteristics (thickness and spatial distribution) might vary substantially along the extreme climatic and geomorphological gradient of HMA. And yet, cliffs and ponds do appear to form on most of the *region's debris-covered glaciers*, from the stagnant tongues of central Himalayan glaciers to the much more active, winter

accumulation Karakoram glaciers. This is an important field of future investigation that will need to be addressed to understand debris-covered glaciers mass balance and dynamics. It can substantially benefit from the availability of new high resolution satellite images and very high resolution UAV surveys, as we have shown that high resolution topographical information of both the cliff and surrounding glacier surface is crucial to understand and correctly represent cliff backwasting patterns.

Materials and Methods

We mapped two supraglacial ice cliffs on the debris-covered tongue of Lirung Glacier (Langtang Valley, Nepalese Himalaya) using a high-resolution orthoimage and digital elevation model (DEM), which were derived from an unmanned aerial vehicle (UAV) survey in May 2013 (21). No south-facing cliffs were observed on Lirung Glacier (nor on the other glaciers of Langtang valley). Therefore we rotated the two cliffs including their surrounding topography and ponds (within 100m in xy-direction) by applying a 2D-matrix rotation around a common center coordinate. The rotation angle

is defined as the deviation between the observed mean cliff aspect and the target direction in degrees. For our simulations we selected two observed cliffs of different size (one relatively large and one relatively small), aspect (northeast and northwest) and bottom configuration (in contact with a supraglacial pond and with no water contact). Both were located within 100m from an on-glacier automatic weather station (AWS), which allowed forcing the cliff energy balance and backwasting model with local, high resolution and accurate meteorological input.

A physically-based, dynamic 3D-backwasting model (14), which has previously been tested for four cliffs (of which two are investigated in this study) on the same glacier and for the same period, allowed us to test the behaviour of the south-facing cliffs generated by rotation of the two original cliffs. The model has been validated for the two original cliffs with multiple independent data sets (14), lending confidence to its use for this experiment. For this study, we further improved the model algorithm for more stable and computationally efficient simulations (SI, Section 3). The use of a high-resolution DEM for initial conditions and hourly meteorological data recorded on-glacier allow the model to calculate radiation and shading at the cliff surface with very high level of detail (11). Simulated melt from calculation of the cliff surface energy balance (SI, Section 3.A) was accumulated for every cliff cell over two-week intervals, after which the cliff geometry was updated accordingly (14) (SI, Section 3.D). Enhanced melt rates were applied to cliff sections in direct contact with ponded water (14), accounting for thermo-erosion (10) (SI, Section 3.J). The model algorithm also considered expansion and shrinkage of marginal cliff zones based on slope and debris-view thresholds as described in (14) and in the SI (Sections 3.G,H).

To provide the context of our modelling experiment, we mapped supraglacial cliffs and ponds on both Lirung Glacier and the much larger Langtang Glacier, the largest and most remote glacier in the Langtang catchment ((7), Fig. S10). We have used a UAV-survey from May 2014 (orthoimage and DEM with 0.1m and 0.2m spatial resolution, respectively) and SPOT6-imagery from April 2014 (orthoimage and DEM with 1.5m and 3m spatial resolution, respectively) to delineate supraglacial ice cliffs and ponds and to derive their initial topographies. Mapping was carried out manually, based on visual interpretation using the high resolution orthoimages and topography (slope) information (SI, Section 5.A) (7). We used these inventories to determine the distribution of southerly-facing cliffs within the total cliff distribution on both glaciers. We then applied the 3D ice cliff ablation and backwasting model (SI, Section 3) to all the cliffs on the two glaciers to calculate the volume losses associated with all cliffs, and specifically south-facing cliffs, respectively, over one ablation season. We use a fully distributed, physically-based glacio-hydrological model (TOPKAPI-ETH) run over the same period and the same spatial domain to calculate the mass losses of the two glaciers (SI, Section 5.A). The models are run with meteorological input data from AWSs on-glacier and in the valley, extrapolated to each single cliff location with local lapse rates (SI, Section 5.A). Radiative fluxes are modelled (SI, Sections 3.A,B) and cliff geometries are updated (SI, Section 3.D) two times during the melt season.

ACKNOWLEDGMENTS. This study is funded by the SNF (Swiss National Science Foundation) project UNCOMUN (“Understanding Contrasts in High Mountain Hydrology in Asia”, Grant No. 146761). We would like to thank very much two anonymous reviewers that have provided very thorough and constructive reviews that have contributed to improve the manuscript.

5. Gardelle J, Berthier E, Arnaud Y (2012) Slight mass gain of Karakoram glaciers in the early twenty-first century. *Nature Geosci* 5(5):322–325.
6. Kääb A, Berthier E, Nuth C, Gardelle J, Arnaud Y (2012) Contrasting patterns of early twenty-first-century glacier mass change in the Himalayas. *Nature* 488(7412):495–8.
7. Ragettli S, Bolch T, Pellicciotti F (2016) Heterogeneous glacier thinning patterns over the last 40 years in Langtang Himal, Nepal. *The Cryosphere* 10(5):2075–2097.
8. Vincent C, et al. (2016) Reduced melt on debris-covered glaciers: investigations from Changri Nup Glacier, Nepal. *The Cryosphere* 10(4):1845–1858.
9. Sakai A, Takeuchi N, Fujita K, Nakawo M (2000) Role of supraglacial ponds in the ablation process of a debris-covered glacier in the Nepal Himalayas. *IAHS Publ.* 265 pp. 119–132.
10. Miles ES, et al. (2016) Refined energy-balance modelling of a supraglacial pond, Langtang Khola, Nepal. *Annals of Glaciology* 57(71):29–40.
11. Buri P, Pellicciotti F, Steiner JF, Miles ES, Immerzeel WW (2016a) A grid-based model of backwasting of supraglacial ice cliffs on debris-covered glaciers. *Annals of Glaciology* 57(71):199–211.
12. Thompson S, Benn DI, Mertes J, Luckman A (2016) Stagnation and mass loss on a Himalayan debris-covered glacier: processes, patterns and rates. *Journal of Glaciology* 62(233):467–485.
13. Rowan AV, Egholm DL, Quincey DJ, Glasser NF (2015) Modelling the feedbacks between mass balance, ice flow and debris transport to predict the response to climate change of debris-covered glaciers in the Himalaya. *Earth and Planetary Science Letters* 430:427–438.
14. Buri P, et al. (2016b) A physically based 3-D model of ice cliff evolution over debris-covered glaciers. *Journal of Geophysical Research: Earth Surface* 121(12):2471–2493.
15. Brun F, et al. (2016) Quantifying volume loss from ice cliffs on debris-covered glaciers using high-resolution terrestrial and aerial photogrammetry. *Journal of Glaciology* pp. 1–12.
16. Sakai A, Nakawo M, Fujita K (2002) Distribution characteristics and energy balance of ice cliffs on debris-covered glaciers, Nepal Himalaya. *Arctic, Antarctic, and Alpine Research* pp. 12–19.
17. Inoue J, Yoshida M (1980) Ablation and heat exchange over the Khumbu Glacier. *Journal of the Japanese Society of Snow and Ice* 41(Special):26–33.
18. Sakai A, Nakawo M, Fujita K (1998) Melt rate of ice cliffs on the Lirung glacier, Nepal Himalayas, 1996. *Bull. Glacier Res* 16:57–66.
19. Brun CS, Quincey DJ, Carrivick JL, Smith MW (2017) Ice cliff dynamics in the Everest region of the Central Himalaya. *Geomorphology* 278:238–251.
20. Steiner J, et al. (2015) Modeling ice cliff backwasting on a debris covered glacier in the Nepalese Himalayas. *Journal of Glaciology* 61(229):889–907.
21. Immerzeel W, et al. (2014) High-resolution monitoring of Himalayan glacier dynamics using unmanned aerial vehicles. *Remote Sensing of Environment* 150:93–103.
22. Fujita K, Sakai A, Chhetri T (1997) Meteorological observation in Langtang Valley, Nepal Himalayas, 1996. *Bulletin of Glacier Research* 15:71–78.
23. Immerzeel W, Petersen L, Ragettli S, Pellicciotti F (2014) The importance of observed gradients of air temperature and precipitation for modeling runoff from a glacierized watershed in the Nepalese Himalayas. *Water Resources Research* 50(3):2212–2226.
24. Pellicciotti F, et al. (2015) Mass-balance changes of the debris-covered glaciers in the Langtang Himal, Nepal, 1974–99. *Journal of Glaciology* 61(226):373–386.
25. Kirkbride MP (1993) The temporal significance of transitions from melting to calving termini at glaciers in the central Southern Alps of New Zealand. *The Holocene* 3(3):232–240.
26. Benn DI, et al. (2012) Response of debris-covered glaciers in the Mount Everest region to recent warming, and implications for outburst flood hazards. *Earth-Science Reviews* 114(1–2):156–174.

1. Scherler D, Bookhagen B, Strecker M (2011) Spatially variable response of Himalayan glaciers to climate change affected by debris cover. *Nature Geoscience* 4(3):156–159.
2. Bolch T, et al. (2012) The state and fate of Himalayan glaciers. *Science* 336(6079):310–314.
3. Østrem G (1959) Ice melting under a thin layer of moraine, and the existence of ice cores in moraine ridges. *Geografiska Annaler* 41(4):228–230.
4. Evatt GW, et al. (2015) Glacial melt under a porous debris layer. *Journal of Glaciology* 61(229):825–836.